DYNAMIC RESPONSE SENSITIVITY OF INELASTIC STRUCTURES

By

Yan Zhang
Armen Der Kiureghian

A report on research supported by
the National Science Foundation under
Grant No. MSM-8922077

Report No. UCB/SEMM-91/06
Structural Engineering, Mechanics and Materials Program
Department of Civil Engineering
University of California
Berkeley, California, U.S.A.

October 1991

Abstract

A general finite element solution method for the dynamic response sensitivity of inelastic structures is developed. Employing conditional derivatives, the gradient equation of motion is solved without iteration and by taking advantage of the available solution of the response. Special attention is given to sensitivities with respect to inelastic material parameters and detailed derivations are made for the J_2 plasticity model with linear hardening rule. The method can be generally applied to any other inelastic material models that have analytically defined yield function and flow rule. The formulation is easily incorporated in existing finite element codes. Numerical examples demonstrate the accuracy and efficiency of the method.

Acknowledgment

This work was supported by Grant Number MSM-8922077 from the National Science Foundation with Dr. Ken Chong as Program Director. This support is gratefully acknowledged. The authors wish to thank Professors J. Lubliner and R. L. Taylor for their comments on an earlier version of the manuscript.

Contents

1 Introduction

Response sensitivity analysis aims at measuring the rate of variation in the response of a structure with respect to parameters describing, e.g., the material of the structure, its geometry or the applied loads. Measures of sensitivity in general are expressed in terms of the partial derivatives of the response with respect to the parameters of interest, i.e., the gradient. These measures are useful in a variety of applications, including the determination of relative importance of parameters, optimum structural design, design of experiments, optimum allocation of resources, and probabilistic analysis.

The authors' interest in this field stems from their work in probabilistic analysis. In such analysis, the gradients of the response with respect to uncertain variables are used either for estimating the response variability in a second-moment context (e.g., determining the variance of the response for prescribed means and variance/covariances of the uncertain variables), or for determining the probability of exceeding a prescribed limit state, commonly known as reliability analysis [13]. In such applications, the uncertain quantities usually are the material properties of the structure, the applied loads, and the geometry or boundary of the structure. In reliability analysis, as in optimum design, the gradients are used to determine a direction of search in an iterative algorithm for finding an optimum solution point [10]. Both accuracy and efficiency of the gradient computation are required to ensure rapid convergence of the search algorithm.

Several general methods are available for computing the gradients of structural response. A comprehensive review is made by Haftka and Adelman [6]. The most straightforward approach is using finite differences. This requires repeated solutions of the problem at least one time greater than the number of sensitivity parameters. The accuracy depends on the difference formulation used and on the choice of the finite variation in the sensitivity parameter. A computationally more efficient approach employs perturbation analysis [11, 7]. In this, the governing equation of the response for a perturbed value of the sensitivity parameter is expanded and, after deleting higher-order terms, an equation for the corresponding perturbation in the response is derived which has a form similar to the equation of the response itself. In solving the perturbed equation, advantage is taken of the available solution of the response and a complete reanalysis is not necessary. The accuracy depends on the size of the perturbation used and on the importance of the neglected higher-order terms. In general, the perturbation method is less accurate but more efficient than the finite-difference method. Iterative methods that improve the efficiency or accuracy of the above approximate methods have also been suggested [5, 4]. In terms of accuracy and efficiency, these methods lie somewhere between the finite difference and perturbation methods.

An alternative approach for computing the response gradients is to directly differentiate the equation governing the response with respect to the variable of interest. The result is an equation for the gradient which has a form similar to the equation of the response itself. Thus, this approach enjoys the same advantage of efficiency as the perturbation method, but it is accurate as it employs no approximation, save for the approximation involved in the numerical solution of the equations of the response and the gradient. This approach has been called the Direct Differentiation Method (DDM) [17]. The objective of this paper is to present a new, general formulation with this approach for the dynamic response of structures with inelastic material. Detailed formulations are developed for materials with the J_2 plasticity constitutive law. Particular attention is given to the response gradients with respect to the inelastic material property constants. Although such gradients may be of limited interest in optimum design applications, they are of prime interest in reliability analysis where the material property constants are often treated as random variables to account for the underlying uncertainties.

The DDM has been applied to elastic and inelastic problems by previous researchers [14, 8, 2, 17, 9]. For inelastic problems, the difficulty lies in the internal resisting forces, which are history dependent and have implicit relations with the sensitivity parameters. Ray et al. [14] developed formulations for the response gradients of hysteretic dynamic frame systems with respect to member cross-sectional areas. The formulation is not in a conventional finite element form and it is not clear that it can be readily applied to compute the sensitivities with respect to inelastic material property constants, such as the yield stress. More recently, general formulations for both geometrically and materially nonlinear problems were proposed [2, 17]. Examples were used to show that the formulations could be implemented in a finite element context [2, 1, 16]. However, as in the method of Ray et al., it is not clear that their approaches are applicable to the response gradients with respect to inelastic material property constants for general structures.

The alternative direct differentiation method proposed here is different from the above formulations in the manner of computing the gradient of the resisting forces. Rather than directly computing the total derivative, the formulation employs the partial derivatives with respect to the sensitivity parameter and the present value of the displacement vector. The resulting equation of the gradient naturally involves the tangent stiffness matrix, which is available from the solution of the response if a Newton-type algorithm is used, and this facilitates the solution of the gradient equation. The partial derivative of the resisting forces with respect to the sensitivity parameter is obtained in terms of the derivatives of the constitutive equations of the material for fixed values of the displacements. The proposed method is referred to as the Conditional Derivative Method (CDM). Although the derivations here are fully developed only for the J_2 plasticity law, the procedure is general and can be developed for other models of inelastic material.

The proposed method has been implemented in the finite element code FEAP by R. L. Taylor [19] and a number of applications have been carried out. The present paper concludes with the presentation of two numerical examples: a perforated strip under plane strain and a truss structure under dynamic loading, both having plastic materials with hardening. Comparisons with finite-difference results demonstrate the accuracy of the procedure and estimates of computer execution time provide indications of its efficiency.

2 The Conditional Derivative Method

Let x denote a parameter, with respect to which response sensitivities are of interest. x may denote a material property constant (e.g., a modulus, yield stress, hardening parameter, certain geometry parameters) or a load parameter. We consider the class of nonlinear dynamic problems for which the equation of motion can be written in the form

$$\boldsymbol{M}(x)\ddot{\boldsymbol{u}}(t,x) + \boldsymbol{C}(x)\dot{\boldsymbol{u}}(t,x) + \boldsymbol{R}(\boldsymbol{u}(t,x),x) = \boldsymbol{P}(t,x) \tag{1}$$

where t denotes the time, $\boldsymbol{u}(t,x)$ denotes the displacement vector, $\boldsymbol{M}(x)$ is the mass matrix, $\boldsymbol{C}(x)$ is the damping matrix, $\boldsymbol{R}(\boldsymbol{u}(t,x),x)$ denotes the internal resisting force vector, and $\boldsymbol{P}(t,x)$ denotes the external load vector, and a superposed dot indicates differentiation with respect to time. The dependences of $\boldsymbol{R}$ on the current value of the displacement vector and the sensitivity parameter are explicitly shown. However, for an inelastic problem, $\boldsymbol{R}$ is also history dependent. Although this dependence is not explicitly shown in this formulation, it is implied and will be accounted for through the constitutive equations to be developed in the following section.

The equation for the response gradient $\boldsymbol{v} = \frac{\partial \boldsymbol{u}}{\partial x}$ is obtained by directly differentiating Eq. 1 with respect to x. After changing the orders of differentiation with respect to t and x and rearranging terms, one obtains

$$\boldsymbol{M}\ddot{\boldsymbol{v}} + \boldsymbol{C}\dot{\boldsymbol{v}} + \boldsymbol{K}(\boldsymbol{u})\boldsymbol{v} = \frac{\partial \boldsymbol{P}}{\partial x} - \frac{\partial \boldsymbol{M}}{\partial x}\ddot{\boldsymbol{u}} - \frac{\partial \boldsymbol{C}}{\partial x}\dot{\boldsymbol{u}} - \left.\frac{\partial \boldsymbol{R}}{\partial x}\right|_{\boldsymbol{u}} \tag{2}$$

in which $\boldsymbol{K}(u) = \frac{\partial \boldsymbol{R}}{\partial \boldsymbol{u}}$ is the current tangent stiffness matrix. The vector $\left.\frac{\partial \boldsymbol{R}}{\partial x}\right|_{\boldsymbol{u}}$ represents the derivative of the resisting forces with respect to x with $\boldsymbol{u}$ fixed. It depends on the assumed constitutive law of the material and is history dependent.

The response and its gradient are obtained by successively solving Eqs. 1 and 2. For known $\boldsymbol{u}$, Eq. 2 for the gradient $\boldsymbol{v}$ is linear, although the coefficient matrix $\boldsymbol{K}(\boldsymbol{u})$ in general may depend on t. This linearity is one advantage of CDM. It will become more apparent when a step-by-step algorithm is used to solve the set of equations.

In a finite element setting, the resisting force vector is given by [19]

$$\boldsymbol{R}(\boldsymbol{u}, x) = \sum_{e} \int_{\Omega_e} \boldsymbol{B}\boldsymbol{\sigma}(\boldsymbol{\varepsilon}, x) d\Omega \tag{3}$$

where e denotes the element number and the summation is over all the elements in the structure, Ω_e is the domain of the element, $\boldsymbol{B}$ is the discrete strain operator, and $\boldsymbol{\sigma}(\boldsymbol{\varepsilon}, x)$ is the stress vector, which is expressed as a function of the strain vector $\boldsymbol{\varepsilon}$ and x. Again, the history-dependence of the stress vector is not shown explicitly in this formulation, but it is implied. Taking derivative with respect to x with $\boldsymbol{u}$ fixed, one obtains

$$\left.\frac{\partial \boldsymbol{R}}{\partial x}\right|_{\boldsymbol{u}} = \sum_{e} \int_{\Omega_e} \boldsymbol{B} \left.\frac{\partial \boldsymbol{\sigma}}{\partial x}\right|_{\boldsymbol{\varepsilon}} d\Omega \tag{4}$$

where $\left.\frac{\partial \boldsymbol{\sigma}}{\partial x}\right|_{\boldsymbol{\varepsilon}}$ is the derivative with respect to x with the strains fixed. This equation assumes that the boundary of the element is not a function of x.

Normally a step-by-step numerical integration method is used to solve Eq. 1 at discrete time steps $t = t_n$ for $n = 0, 1, 2, \ldots$. The class of one-step implicit integration methods approximate the acceleration and velocity at t_{n+1} by

$$\ddot{\boldsymbol{u}}_{n+1} = a_0 \boldsymbol{u}_{n+1} - a_2 \boldsymbol{u}_n - a_4 \dot{\boldsymbol{u}}_n - a_6 \ddot{\boldsymbol{u}}_n \tag{5}$$

$$\dot{\boldsymbol{u}}_{n+1} = a_1\boldsymbol{u}_{n+1} - a_3\boldsymbol{u}_n - a_5\dot{\boldsymbol{u}}_n - a_7\ddot{\boldsymbol{u}}_n \tag{6}$$

where a_0-a_7 are the integration coefficients which depend on the particular method used. Substituting the above approximations into Eq. 1 at time t_{n+1}, results in

$$a_0\boldsymbol{M}\boldsymbol{u}_{n+1} + a_1\boldsymbol{C}\boldsymbol{u}_{n+1} + \boldsymbol{R}(\boldsymbol{u}_{n+1}) = \tilde{\boldsymbol{P}}_{n+1} \tag{7}$$

with

$$\tilde{\boldsymbol{P}}_{n+1} = \boldsymbol{P}_{n+1} + \boldsymbol{M}(a_2\boldsymbol{u}_n + a_4\dot{\boldsymbol{u}}_n + a_6\ddot{\boldsymbol{u}}_n) + \boldsymbol{C}(a_3\boldsymbol{u}_n + a_5\dot{\boldsymbol{u}}_n + a_7\ddot{\boldsymbol{u}}_n) \tag{8}$$

being the effective loading at step $n+1$. The most common algorithm for solving Eq. 7 for $\boldsymbol{u}_{n+1}$ is by Newton iteration, which can be summarized by the set of equations

$$[a_0\boldsymbol{M} + a_1\boldsymbol{C} + \boldsymbol{K}(\boldsymbol{u}^i_{n+1})]\triangle\boldsymbol{u}^i_{n+1} = \triangle\boldsymbol{R}(\boldsymbol{u}^i_{n+1}) \tag{9}$$

$$\triangle\boldsymbol{R}(\boldsymbol{u}^i_{n+1}) = \tilde{\boldsymbol{P}}_{n+1} - [a_0\boldsymbol{M}\boldsymbol{u}^i_{n+1} + a_1\boldsymbol{C}\boldsymbol{u}^i_{n+1} + \boldsymbol{R}(\boldsymbol{u}^i_{n+1})] \tag{10}$$

$$\boldsymbol{u}^{i+1}_{n+1} = \boldsymbol{u}^i_{n+1} + \triangle\boldsymbol{u}^i_{n+1} \tag{11}$$

in which $\triangle\boldsymbol{R}(\boldsymbol{u}^i_{n+1})$ is the residual force and $\triangle\boldsymbol{u}^i_{n+1}$ is the incremental displacement at the ith iteration, and $\boldsymbol{u}^{i+1}_{n+1}$ is the updated displacement. One proceeds with the iteration until convergence is reached, resulting in the solution $\boldsymbol{u}_{n+1}$.

The partial derivative equation for the gradient, Eq. 2, is solved in conjunction with Eq. 1 using the same integration procedure. The counterpart of Eq. 7 for the gradient is

$$\begin{aligned}&[a_0\boldsymbol{M} + a_1\boldsymbol{C} + \boldsymbol{K}(\boldsymbol{u}_{n+1})]\boldsymbol{v}_{n+1} = \\ &\quad \frac{\partial\tilde{\boldsymbol{P}}_{n+1}}{\partial x} - [a_0\frac{\partial\boldsymbol{M}}{\partial x}\boldsymbol{u}_{n+1} + a_1\frac{\partial\boldsymbol{C}}{\partial x}\boldsymbol{u}_{n+1} + \left.\frac{\partial\boldsymbol{R}(\boldsymbol{u}_{n+1})}{\partial x}\right|_{\boldsymbol{u}_{n+1}}]\end{aligned} \tag{12}$$

in which

$$\frac{\partial \tilde{\boldsymbol{P}}_{n+1}}{\partial x} = \frac{\partial \boldsymbol{P}_{n+1}}{\partial x} + \tag{13}$$

$$\boldsymbol{M}(a_2 \boldsymbol{v}_n + a_4 \dot{\boldsymbol{v}}_n + a_6 \ddot{\boldsymbol{v}}_n) + \boldsymbol{C}(a_3 \boldsymbol{v}_n + a_5 \dot{\boldsymbol{v}}_n + a_7 \ddot{\boldsymbol{v}}_n) +$$

$$\frac{\partial \boldsymbol{M}}{\partial x}(a_2 \boldsymbol{u}_n + a_4 \dot{\boldsymbol{u}}_n + a_6 \ddot{\boldsymbol{u}}_n) + \frac{\partial \boldsymbol{C}}{\partial x}(a_3 \boldsymbol{u}_n + a_5 \dot{\boldsymbol{u}}_n + a_7 \ddot{\boldsymbol{u}}_n)$$

Observe that the matrix on the left-hand-side of Eq. 12 is identical to that of Eq. 9 at the solution point, $\boldsymbol{u}_{n+1}$. Therefore, only the vectors on the right-hand-side of Eq. 12 need to be computed. The vectors $\frac{\partial \boldsymbol{P}_{n+1}}{\partial x}$, $\frac{\partial \boldsymbol{M}}{\partial x}$ and $\frac{\partial \boldsymbol{C}}{\partial x}$ are normally easy to compute at the element level (see [3]). The vector $\left.\frac{\partial \boldsymbol{R}(\boldsymbol{u}_{n+1})}{\partial x}\right|_{\boldsymbol{u}_{n+1}}$, however, is not easy to compute and requires special treatment, especially in view of the history dependence of $\boldsymbol{R}$. From Eq. 4, the latter vector involves the stress gradient $\left.\frac{\partial \boldsymbol{\sigma}}{\partial x}\right|_{\boldsymbol{\varepsilon}_{n+1}}$, which is dependent on the constitutive law of the material. Computation of this vector is discussed in the following section for materials having the J_2 plasticity constitutive relations. It is worth noting that Eq. 4 is analogous in form to Eq. 3. Therefore, in the finite-element implementation, the procedure used to form the vector $\boldsymbol{R}(\boldsymbol{u})$ can also be used to form the gradient vector $\left.\frac{\partial \boldsymbol{R}(\boldsymbol{u})}{\partial x}\right|_{\boldsymbol{u}}$, which facilitates the implementation.

3 Constitutive Relations of J_2 Plasticity

Consider an isotropic material with plastic constitutive relations. Using a matrix notation, let the total stresses and strains be decomposed as

$$\boldsymbol{\sigma} = p\mathbf{1} + \boldsymbol{s} \quad \text{and} \quad \boldsymbol{\varepsilon} = \frac{1}{3}\theta\mathbf{1} + \boldsymbol{e} \tag{14}$$

where $p = \frac{1}{3}(\sigma_1 + \sigma_2 + \sigma_3)$ and $\theta = \varepsilon_1 + \varepsilon_2 + \varepsilon_3$ are the mean stress and the trace of strain matrix, respectively, $\boldsymbol{s}$ and $\boldsymbol{e}$ are the deviatoric stress and strain vectors, respectively, and $\mathbf{1} = (1, 1, 1, 0, 0, 0)^T$. A complete inelastic model consists of a yield criterion and flow and hardening rules. In this paper we consider the J_2 plasticity model, for which the constitutive relations are given in the rate form [12]

$$\dot{p} = K\dot{\theta} \tag{15}$$

$$\dot{\boldsymbol{s}} = 2G(\dot{\boldsymbol{e}} - \dot{\boldsymbol{e}}^p) \tag{16}$$

where K and G are the bulk and shear modulus, respectively, which are given in terms of the elastic modulus, E, and the Poisson's ratio, ν, by

$$K = \frac{1}{3}\frac{E}{1-2\nu} \quad \text{and} \quad G = \frac{E}{2(1+\nu)} \tag{17}$$

and $\dot{\boldsymbol{e}}^p$ is the plastic strain rate vector given by

$$\dot{\boldsymbol{e}}^p = \dot{\lambda}\frac{\partial F}{\partial \boldsymbol{s}} \tag{18}$$

In the preceding equation, $\dot{\lambda}$ denotes the rate factor and F is the yield function defined by

$$F(\boldsymbol{s}, \boldsymbol{\rho}, \kappa) = f(\boldsymbol{s} - \boldsymbol{\rho}(\boldsymbol{e}^p)) - k(\kappa) \tag{19}$$

in which $\boldsymbol{\rho}(\boldsymbol{e}^p)$ is a vector describing the kinematic hardening, κ is an isotropic hardening variable, and $f(.)$ is the Euclidean norm of the vector $\boldsymbol{\xi} = \boldsymbol{s} - \boldsymbol{\rho}$,

$$f(\boldsymbol{s} - \boldsymbol{\rho}(\boldsymbol{e}^p)) = \|\boldsymbol{\xi}\| = \sqrt{(\boldsymbol{\xi}, \boldsymbol{\xi})} \tag{20}$$

where $(\boldsymbol{\xi}, \boldsymbol{\xi})$ denotes the inner product. The isotropic hardening variable, κ, is usually taken to be the effective plastic strain defined by

$$\bar{e}^p = \int_0^t \sqrt{\frac{2}{3}(\dot{\boldsymbol{e}}^p, \dot{\boldsymbol{e}}^p)}\, dt \tag{21}$$

For the analysis in this paper, we consider the special case of linear kinematic and isotropic hardening rules. In that case, $\boldsymbol{\rho}$ and k in Eq. 18 are given by

$$\boldsymbol{\rho} = \frac{2}{3} H_{kin} \boldsymbol{e}^p \tag{22}$$

$$k(\kappa) = \sqrt{\frac{2}{3}}(\sigma_y + H_{iso}\bar{e}^p) \tag{23}$$

where H_{kin} and H_{iso} are the kinematic and isotropic hardening parameters, respectively, and σ_y is the yield stress. This completes the definition of the plasticity model used in the remainder of this paper.

In the incremental solution procedure, the above rate equations are usually discretized by the backward Euler method. The set of discretized rate equations at time t_{n+1} then reads as follows:

$$p_{n+1} = K\theta_{n+1} \tag{24}$$

$$\boldsymbol{s}_{n+1} = 2G(\boldsymbol{e}_{n+1} - \boldsymbol{e}^p_{n+1}) \tag{25}$$

$$\boldsymbol{e}^p_{n+1} = \boldsymbol{e}^p_n + \triangle\lambda_{n+1}\boldsymbol{n}_{n+1} \quad \text{with} \quad \boldsymbol{n}_{n+1} = \frac{\boldsymbol{\xi}_{n+1}}{||\boldsymbol{\xi}_{n+1}||} \tag{26}$$

$$\bar{e}^p_{n+1} = \bar{e}^p_n + \sqrt{\frac{2}{3}}\triangle\lambda_{n+1} \tag{27}$$

where $\boldsymbol{n}_{n+1}$ is a unit vector normal to the yield surface at time t_{n+1}. In addition, when plastic deformation occurs, the consistency condition requires that

$$||\boldsymbol{\xi}_{n+1}|| - k_{n+1} = 0 \tag{28}$$

with

$$\boldsymbol{\xi}_{n+1} = \boldsymbol{s}_{n+1} - \frac{2}{3}H_{kin}\boldsymbol{e}^p_{n+1} \quad \text{and} \quad k_{n+1} = \sqrt{\frac{2}{3}}(\sigma_y + H_{iso}\bar{e}^p_{n+1}) \tag{29}$$

The above set of equations can be solved in conjunction with Eq. 7 by use of a procedure such as the return map algorithm [15] .

4 Gradient of Constitutive Relations

The gradient equations of the constitutive relations are obtained by taking derivatives of Eqs. 24 - 29 with respect to x, producing the following

$$\frac{\partial p_{n+1}}{\partial x} = \frac{\partial K}{\partial x}\theta_{n+1} + K\frac{\partial \theta_{n+1}}{\partial x} \tag{30}$$

$$\frac{\partial s_{n+1}}{\partial x} = 2\frac{\partial G}{\partial x}(\boldsymbol{e}_{n+1} - \boldsymbol{e}^p_{n+1}) + 2G(\frac{\partial \boldsymbol{e}_{n+1}}{\partial x} - \frac{\partial \boldsymbol{e}^p_{n+1}}{\partial x}) \tag{31}$$

$$\frac{\partial \boldsymbol{e}^p_{n+1}}{\partial x} = \frac{\partial \boldsymbol{e}^p_n}{\partial x} + \frac{\partial \triangle\lambda_{n+1}}{\partial x}\boldsymbol{n}_{n+1} + \triangle\lambda_{n+1}\frac{\partial \boldsymbol{n}_{n+1}}{\partial x} \tag{32}$$

$$\frac{\partial \boldsymbol{n}_{n+1}}{\partial x} = \frac{1}{||\boldsymbol{\xi}_{n+1}||}(\boldsymbol{I} - \boldsymbol{n}_{n+1}\boldsymbol{n}^T_{n+1})\frac{\partial \boldsymbol{\xi}_{n+1}}{\partial x} \tag{33}$$

$$\frac{\partial \bar{e}^p_{n+1}}{\partial x} = \frac{\partial \bar{e}^p_n}{\partial x} + \sqrt{\frac{2}{3}}\frac{\partial \triangle\lambda_{n+1}}{\partial x} \tag{34}$$

$$\boldsymbol{n}^T_{n+1}\frac{\partial \boldsymbol{\xi}_{n+1}}{\partial x} - \frac{\partial k_{n+1}}{\partial x} = 0 \qquad for \quad F_{n+1} = 0 \tag{35}$$

$$\frac{\partial \boldsymbol{\xi}_{n+1}}{\partial x} = \frac{\partial s_{n+1}}{\partial x} - \frac{2}{3}(\frac{\partial H_{kin}}{\partial x}\boldsymbol{e}^p_{n+1} + H_{kin}\frac{\partial \boldsymbol{e}^p_{n+1}}{\partial x}) \tag{36}$$

$$\frac{\partial k_{n+1}}{\partial x} = \sqrt{\frac{2}{3}}(\frac{\partial \sigma_y}{\partial x} + \frac{\partial H_{iso}}{\partial x}\bar{e}^p_{n+1} + H_{iso}\frac{\partial \bar{e}^p_{n+1}}{\partial x}) \tag{37}$$

where $\boldsymbol{I}$ is the identity matrix. The above equations are valid for both elastic and plastic deformations, except for the condition in Eq. 35 that applies only when plastic deformation occurs, i.e., when the yield function at the step is zero. Note that under elastic deformation, $\triangle\lambda_{n+1}$ and its gradient are both zero and Eqs. 32 and 34 can be simplified. In the present analysis, the parameter x is assumed to be one of the constants K, G, H_{kin}, H_{iso} or σ_y.

Then, the gradient terms $\frac{\partial K}{\partial x}$, $\frac{\partial G}{\partial x}$, $\frac{\partial H_{kin}}{\partial x}$, $\frac{\partial H_{iso}}{\partial x}$, and $\frac{\partial \sigma_y}{\partial x}$ are either one or zero, depending on the choice of x.

As can be seen in Eq. 32, the solutions of $\frac{\partial \boldsymbol{n}_{n+1}}{\partial x}$ and $\frac{\partial \triangle\lambda_{n+1}}{\partial x}$ are essential for determining the gradient of the plastic strain. In order to derive expressions for these quantities, we first solve for $\frac{\partial \boldsymbol{\xi}_{n+1}}{\partial x}$ by substituting Eqs. 31 and 32 into Eq. 36. After some algebra, the result is

$$\begin{aligned} \frac{\partial \boldsymbol{\xi}_{n+1}}{\partial x} &= -(2G + \frac{2}{3}H_{kin})(\frac{\partial \boldsymbol{e}^p_n}{\partial x} + \frac{\partial \triangle\lambda_{n+1}}{\partial x}\boldsymbol{n}_{n+1} + \triangle\lambda_{n+1}\frac{\partial \boldsymbol{n}_{n+1}}{\partial x}) + \\ & 2G\frac{\partial \boldsymbol{e}_{n+1}}{\partial x} - \frac{2}{3}\frac{\partial H_{kin}}{\partial x}\boldsymbol{e}^p_{n+1} \end{aligned} \tag{38}$$

Substituting this result into Eq. 33, after some lengthy manipulations, we obtain

$$\begin{aligned} \frac{\partial \boldsymbol{n}_{n+1}}{\partial x} &= \frac{1}{\|\boldsymbol{\xi}_{n+1}\| + (2G + \frac{2}{3}H_{kin})\triangle\lambda_{n+1}}(\boldsymbol{I} - \boldsymbol{n}_{n+1}\boldsymbol{n}^T_{n+1}) + \\ & [-(2G + \frac{2}{3}H_{kin})\frac{\partial \boldsymbol{e}^p_n}{\partial x} - \frac{2}{3}\frac{\partial H_{kin}}{\partial x}\boldsymbol{e}^p_{n+1} + \\ & 2G\frac{\partial \boldsymbol{e}_{n+1}}{\partial x} + 2\frac{\partial G}{\partial x}(\boldsymbol{e}_{n+1} - \boldsymbol{e}^p_{n+1})] \qquad for \quad F_{n+1} = 0 \\ &= 0 \qquad for \quad F_{n+1} < 0 \end{aligned} \tag{39}$$

In deriving this expression, use has been made of the identities $(\boldsymbol{I} - \boldsymbol{n}\boldsymbol{n}^T)\boldsymbol{n} = 0$ and $(\boldsymbol{I} - \alpha\boldsymbol{n}\boldsymbol{n}^T)^{-1} = \boldsymbol{I} + \frac{\alpha}{1-\alpha}\boldsymbol{n}\boldsymbol{n}^T$ involving the unit normal vector $\boldsymbol{n}$. Observe that the only unknown on the right-hand side of the above expression is the gradient of the deviatoric strain at step $n+1$. Note also that the expression involves the gradient of the plastic strain from the previous step, which shows the history dependence of the solution. For $F_{n+1} < 0$, obviously $\frac{\partial \boldsymbol{n}_{n+1}}{\partial x} = 0$ since no plastic deformation occurs.

To derive an expression for $\frac{\partial \triangle\lambda_{n+1}}{\partial x}$, we substitute Eqs. 34 and 39 into Eqs. 37 and 38, respectively, and then substitute the results into Eq. 35 . After extensive algebra and use of the above mentioned identities, the result is

$$
\begin{aligned}
\frac{\partial \triangle\lambda_{n+1}}{\partial x} &= \frac{1}{2G+\frac{2}{3}H_{kin}+\frac{2}{3}H_{iso}}\{\boldsymbol{n}_{n+1}^T[-(2G+\frac{2}{3}H_{kin})\frac{\partial \boldsymbol{e}_n^p}{\partial x} - \\
& \frac{2}{3}\frac{\partial H_{kin}}{\partial x}\boldsymbol{e}_{n+1}^p + 2G\frac{\partial \boldsymbol{e}_{n+1}}{\partial x} + 2\frac{\partial G}{\partial x}(\boldsymbol{e}_{n+1}-\boldsymbol{e}_{n+1}^p)] - \\
& \sqrt{\frac{2}{3}}(\frac{\partial \sigma_y}{\partial x} + \frac{\partial H_{iso}}{\partial x}\bar{e}_{n+1}^p + H_{iso}\frac{\partial \bar{e}_n^p}{\partial x})\} \qquad for \quad F_{n+1}=0 \\
&= 0 \qquad for \quad F_{n+1}<0
\end{aligned} \tag{40}
$$

Observe again that the only unknown term on the right-hand side is the gradient of the deviatoric strain at step $n+1$. For $F_{n+1}<0$, $\frac{\partial \triangle\lambda_{n+1}}{\partial x}=0$ since no plastic deformation occurs.

Now consider the gradient of the stress vector, $\boldsymbol{\sigma}$. Using Eqs. 14, 30 and 31, on obtains

$$
\begin{aligned}
\frac{\partial \boldsymbol{\sigma}_{n+1}}{\partial x} &= \boldsymbol{1}\frac{\partial p_{n+1}}{\partial x} + \frac{\partial \boldsymbol{s}_{n+1}}{\partial x} \\
&= \boldsymbol{1}(\frac{\partial K}{\partial x}\theta_{n+1} + K\frac{\partial \theta_{n+1}}{\partial x}) + 2\frac{\partial G}{\partial x}(\boldsymbol{e}_{n+1}-\boldsymbol{e}_{n+1}^p) + 2G(\frac{\partial \boldsymbol{e}_{n+1}}{\partial x} - \frac{\partial \boldsymbol{e}_{n+1}^p}{\partial x})
\end{aligned} \tag{41}
$$

As noted in Eq. 4 and the discussion following Eqs. 12 and 13, the quantity needed in order to solve Eq. 12 for $\boldsymbol{v}_{n+1}$ is the gradient of $\boldsymbol{\sigma}$ with $\boldsymbol{\varepsilon}_{n+1}$ fixed. This is obtained simply by setting the terms $\frac{\partial \theta_{n+1}}{\partial x}$ and $\frac{\partial \boldsymbol{e}_{n+1}}{\partial x}$ in the preceding equation to be zero. The result is

$$
\left.\frac{\partial \boldsymbol{\sigma}_{n+1}}{\partial x}\right|_{\boldsymbol{\varepsilon}_{n+1}} = \boldsymbol{1}\frac{\partial K}{\partial x}\theta_{n+1} + 2\frac{\partial G}{\partial x}(\boldsymbol{e}_{n+1}-\boldsymbol{e}_{n+1}^p) - 2G\left.\frac{\partial \boldsymbol{e}_{n+1}^p}{\partial x}\right|_{\boldsymbol{e}_{n+1}} \tag{42}
$$

At the solution of the equations of motion (Eq. 7) and the constitutive relations (Eqs. 24-27) at step $n+1$, the only remaining unknown quantity in the preceding equation is $\left.\frac{\partial \boldsymbol{e}_{n+1}^p}{\partial x}\right|_{\boldsymbol{e}_{n+1}}$. Using Eq. 32,

$$
\left.\frac{\partial \boldsymbol{e}_{n+1}^p}{\partial x}\right|_{\boldsymbol{e}_{n+1}} = \frac{\partial \boldsymbol{e}_n^p}{\partial x} + \left.\frac{\partial \triangle\lambda_{n+1}}{\partial x}\right|_{\boldsymbol{e}_{n+1}} \boldsymbol{n}_{n+1} + \triangle\lambda_{n+1}\left.\frac{\partial \boldsymbol{n}_{n+1}}{\partial x}\right|_{\boldsymbol{e}_{n+1}} \tag{43}
$$

The partial derivatives of $\boldsymbol{n}_{n+1}$ and λ_{n+1} are obtained from Eqs. 39 and 40, respectively, by setting the term $\frac{\partial \boldsymbol{e}_{n+1}}{\partial x}$ to be zero, i.e.,

$$\left.\frac{\partial \boldsymbol{n}_{n+1}}{\partial x}\right|_{e_{n+1}} = \frac{1}{\|\boldsymbol{\xi}_{n+1}\| + (2G + \frac{2}{3}H_{kin})\triangle\lambda_{n+1}}(\boldsymbol{I} - \boldsymbol{n}_{n+1}\boldsymbol{n}_{n+1}^T) \\ [-(2G + \frac{2}{3}H_{kin})\frac{\partial \boldsymbol{e}_n^p}{\partial x} - \frac{2}{3}\frac{\partial H_{kin}}{\partial x}\boldsymbol{e}_{n+1}^p + \\ 2\frac{\partial G}{\partial x}(\boldsymbol{e}_{n+1} - \boldsymbol{e}_{n+1}^p)]; \qquad for \quad F_{n+1} = 0 \\ = 0; \qquad for \quad F_{n+1} < 0 \tag{44}$$

$$\left.\frac{\partial \triangle\lambda_{n+1}}{\partial x}\right|_{e_{n+1}} = \frac{1}{2G + \frac{2}{3}H_{kin} + \frac{2}{3}H_{iso}}\{\boldsymbol{n}_{n+1}^T[-(2G + \frac{2}{3}H_{kin})\frac{\partial \boldsymbol{e}_n^p}{\partial x} - \\ \frac{2}{3}\frac{\partial H_{kin}}{\partial x}\boldsymbol{e}_{n+1}^p + 2\frac{\partial G}{\partial x}(\boldsymbol{e}_{n+1} - \boldsymbol{e}_{n+1}^p)] - \\ \sqrt{\frac{2}{3}}(\frac{\partial \sigma_y}{\partial x} + \frac{\partial H_{iso}}{\partial x}\bar{e}_{n+1}^p + H_{iso}\frac{\partial \bar{e}_n^p}{\partial x})\} \qquad for \quad F_{n+1} = 0 \\ = 0 \qquad for \quad F_{n+1} < 0 \tag{45}$$

The above completes the set of equations necessary to solve the gradient of the inelastic response. The specific procedure used is as follows:

1. Solve the incremental equations of motion (Eq. 7) together with the constitutive relations (Eqs. 24-27) at step $n+1$ by use of the return-map algorithm, and compute the quantities $\boldsymbol{n}_{n+1}$, $\triangle\lambda_{n+1}$, $\boldsymbol{e}_{n+1}^p$ and $\bar{e}_{n+1}^p$;
2. Compute Eqs. 43-45 and substitute in Eq. 41 to compute $\left.\frac{\partial \boldsymbol{\sigma}_{n+1}}{\partial x}\right|_{\boldsymbol{\varepsilon}_{n+1}}$;
3. Compute the partial derivative of the resisting forces for step $n+1$ from Eq. 4;
4. Compute the remaining terms on the right-hand side of Eq. 12.
5. Solve the gradient equation (Eq. 12) for $\boldsymbol{v}_{n+1}$ using the factorized form of the matrix $[a_0\boldsymbol{M} + a_1\boldsymbol{C} + \boldsymbol{K}(\boldsymbol{u}_{n+1})]$ available from step 1;

6. Obtain $\frac{\partial e_{n+1}}{\partial x}$ from v_{n+1}, and then solve Eqs. 39 and 40, and update the "unconditional" derivatives in Eqs. 32 and 34 for use in the next step of the analysis;

7. If desired, compute the gradient of the stress vector from Eq. 41.

The above procedure is of course valid for inelastic static problems that are path dependent. The simplified equations for that case can be obtained by setting the integration coefficient a_0 - a_7 in Eqs. 5-13 equal to zero.

The gradient computation method described above can be implemented into any existing nonlinear finite element code with relatively minor modification and extension. In the present study, the program FEAP (Finite Element Analysis Program) by R.L. Taylor [19] was employed. This program has a modular form and is particularly convenient for the development of the needed routines to perform the gradient computation. The main extensions here were at the element level and involved the development of routines to compute the partial derivative matrices for element mass, damping, resisting force, and external loading. Routines for computing the gradient of the resisting forces at the global level and for solving the gradient equations were developed using macro-commands within a subroutine of FEAP intended for new applications. This implementation appears to be no more difficult than the implementation of other less accurate methods [6, 18].

5 Numerical Examples

In this section numerical examples are presented to illustrate the accuracy and efficiency of the proposed method for computing the response gradients. These examples also demonstrate interesting results for the response sensitivities of inelastic structures.

5.1 Example 1 – Perforated Strip Under Cyclic Loading

The first example is an infinitely long rectangular strip with a circular hole, shown in Fig. 1, which is subjected to the quasi-static cyclic loading $p(t)$ in Fig. 2. The inertia and damping forces are assumed to be insignificant. The strip is assumed to have infinite thickness and to be in a state of plane strain. The elastic properties of the material are $E = 10^3 kN/cm^2$ and $\nu = 0.3$, and its plastic properties are $\sigma_y = 1kN/cm^2$, $H_{iso} = 50kN/cm^2$ and $H_{kin} = 50kN/cm^2$. Four-node quadrilateral finite elements are used with the mesh for a quarter of the body as shown in Fig. 3. The step-size $\triangle t = 0.0625s$ is employed in the incremental procedure for solving the equations of motion and the gradient, and a line search at each Newton iteration is performed to stabilize the solution [19]. For the loading in Fig. 2, the displacement u_1 at point A and the stress component σ_{11} at point B in direction x_1, are shown in Figs. 4a and 4b, respectively.

To verify the validity of the procedure and the accuracy of its implementation, the gradients of the displacement at A and the stress at B with respect to the yield stress, σ_y, are considered. Figure 5 shows comparisons of the computed results with the proposed approach (solid curves) with results obtained from finite-difference analysis (broken curves) with decreasing values of the yield stress deviation $\triangle\sigma_y = 0.1, 0.05$, and $0.001\ kN/cm^2$. In each case, the gradient is scaled by the sensitivity variable so that the curves have the same units as the response itself. As can be seen in the figure, the finite-difference results asymptotically approach the results based on the proposed method, thus indicating the validity of the method and the accuracy of its implementation.

Figure 6 compares scaled gradients of the two response quantities with respect to three plastic material parameters, σ_y, H_{kin} and H_{iso}. For a fixed percent variation in each parameter, the displacement response is found to be more sensitive to the yield stress, except towards the end of the loading where greater sensitivity to H_{kin} and H_{iso} is observed in Fig. 6a. For the stress response, much greater sensitivity is found with respect to the yield stress than to the hardening parameters, as can be seen in Fig. 6b.

The first row in Table 1 lists the CPU times spent for this problem on a DEC-System 5500 workstation. The CPU time for each gradient is only about 16 percent of the time for the response. This fraction can be further reduced by storing additional element-level data at the expense of computer storage. Thus, the CPU times in Table 1 are not necessarily optimum and should be regarded as rough estimates of the required effort in computing the gradients.

5.2 Example 2 – Inelastic Truss Structure Under Dynamic Loading

The second example is a truss structure under dynamic loading. The structure and the loading history are show in Figs. 7 and 8, respectively. The geometric nonlinearity due to large displacements is taken into account in formulating the kinematic relations of the truss

[19].

The material of the truss is assumed to follow the J_2 plasticity law with a linear hardening rule. For the one-dimensional case, the constitutive relations are simplied with only one stress component σ, expressed as

$$\sigma = E(\varepsilon - \varepsilon^p)$$

The plastic strain, ε^p, and the isotropic hardening variable, κ, are expressed as

$$\dot{\varepsilon}^p = \dot{\lambda}\frac{\partial F}{\partial \sigma} \quad \text{and} \quad \dot{\kappa} = \mid \dot{\varepsilon}^p \mid$$

where the yield function F is defined as

$$F = \mid \sigma - H_{kin}\varepsilon^p \mid - (\sigma_y + H_{iso}\kappa)$$

Material property constants considered are $E = 30,000 kN/cm^2$, $H_{kin} = 303.03 kN/cm^2$, $H_{iso} = 0$, and $\sigma_y = 12.0 kN/cm^2$, and the material weight density is $0.761 \times 10^{-2} N/cm^3$. The corss-section area of each member is $A = 6cm^2$. The yield stress σ_y and the kinematic hardening parameter H_{kin} of each truss member are considered as the sensitivity variables. The time step size used is $\triangle t = 0.002s$.

Fig. 9 shows the time histories of the vertical displacement at node 2 and the stress σ_1 of member 1. The corresponding gradients with respect to the yield stress of members 1, 2 and 5 and the hardening parameter H_{kin} of member 1, each scaled by the parameter itself, are shown in Fig. 10. It is found that both response quantities are most sensitive to the yield stress in member 1.

The second row in Table 1 lists the CPU times spent for this problem on the DEC-System 5500 workstation. The CPU time for each gradient is again about 16 percent of the time spent for calculating the response. As mentioned earlier, this fraction can be further reduced by storing additional element-level data at the expense of computer storage.

6 Summary and Conclusions

A general finite element solution method for the gradients of dynamic response of inelastic structures is developed. Employing conditional derivatives, the response gradients are computed efficiently, without iterations and by taking advantage of the available solution of the response. Gradients with respect to inelastic material parameters, which are of special interest in reliability analysis and have received limited attention in the past, are evaluated. Specific derivations are made for the widely used J_2 plasticity model with linear hardening rule. The method is general and can be developed for other inelastic materials whose yield function and flow rule can be analytically defined.

The method is implemented in an existing general-purpose finite element code and several numerical examples are analyzed. The execution time for the gradients is found to be a small fraction of the required execution time of the response. Thus, the method is found to be both efficient and practical for use in applications requiring response sensitivities, such as in optimum design or reliability analysis.

References

[1] J.S. Arora and J.B. Cardoso. A design sensitivity analysis principle and its implementation into ADINA. *Computers & Structures*, 32(3/4):691–705, 1989.

[2] K. K. Choi and J. L. T. Santos. Design sensitivity analysis of non-linear structural systems, part I: theory. *Int. J. Num. Meth. Eng.*, 24:2039–2055, 1987.

[3] A. Der Kiureghian. Finite element methods in structural safety studies. In J.T.P. Yao, R. Corotis, C.B. Brown, and F. Moses, editors, *Structural Safety Studies, Proceedings of the Symposium Sponsored by the Structural Division of the American Society of Civil Engineers in Conjunction with the ASCE Convention in Denver, Colorado*, pages 40–52, New York, 1985. American Society of Civil Engineers.

[4] J. B. Dias and S. Nakazawa. An approach to probabilistic finite element analysis using a mixed-iterative formulation. In W.K. Liu, T. Belytschko, M. Lawrence, and T. Cruse, editors, *Computational Probabilistic Methods, Presented at the Joint ASME/SES Applied Mechanics and Engineering Sciences Conference, Berkeley, CA*, pages 75–86, New York, USA, 1988. The American Society of Mechanical Engineers.

[5] R. T. Haftka. Sensitivity calculations for iteratively solved problems. *Int. J. Num. Meth. Eng.*, 21:1535–1546, 1985.

[6] R. T. Haftka and H. M. Adelman. Recent developents in structural sensitivity analysis. *Strut. Opti.*, 1:137–151, 1989.

[7] T. Hisada, H. Noguchi, O. Murayama, and A. Der Kiureghian. Reliability analysis of elasto-plastic dynamic problems. In A. Der Kiureghian and P. Thoft-Christensen, editors, *Reliability and Optimization of Structural Systems '90, Proceedings of the 3rd IFIP WG7.5 Conference, Berkeley, CA*, pages 161–172, Berlin, Germany, 1990. Springer-Verlag.

[8] I. Kaneko and G. Maier. Optimal design of plastic structures under displacement constraints. *Comp. Meth. Appl. Mech. Eng.*, 27:369–391, 1981.

[9] P. L. Liu and A. Der Kiureghian. Finite element reliability of geometrically nonlinear uncertain structures. *J. Eng. Mech.*, 117(8):1806–1825, 1991.

[10] P. L. Liu and A. Der Kiureghian. Optimization algorithms for structural reliability. *Struct. Safety*, 9(3):161–177, 1991.

[11] W.K. Liu, T. Belytschko, and A. Mani. Probabilistic finite elements for nonlinear structural dynamics. *Comp. Meth. Appl. Mech. Eng.*, 56:61–81, 1986.

[12] J. Lubliner. *Plasticity Theory.* Macmillan Publishing Company, New York, 1990.

[13] H. Madsen, S. Krenk, and N. Lind. *Methods of Structural Safety.* Prentice-Hall,Englewood Cliffs,New Jersey, 1986.

[14] D. Ray, K.S. Pister, and E. Polak. Sensitivity analysis for hysteretic dynamic system: Theory and applications. *Comp. Meth. Appl. Mech. Eng.*, 14:179–208, 1978.

[15] J.C. Simo and R.L. Taylor. Consistent tangent operators for rate-independent elastoplasticity. *Comp. Meth. Appl. Mech. Eng.*, 48:101–118, 1985.

[16] J.J. Tsay and J.S. Arora. Optimum design of nonnonlinear structures with path dependent response. *Strut. Opti.*, 1:203–214, 1989.

[17] J.J. Tsay and J.S. Arora. Nonlinear structural design sensitivity analysis for path dependent problems. part 1: General theory. *Comp. Meth. Appl. Mech. Eng.*, 81:183–208, 1990.

[18] C.C. Wu and J.S. Arora. Design sensitivity analysis of nonlinear response using incremental procedure. *AIAA J.*, 258(8):1118–125, 1987.

[19] O.C. Zienkiewicz and R.L. Taylor. *The Finite Element Method*, volume 2. McGraw-Hill, London, 1991.

Table 1: Comparision of Execution Times for Gradients

	total cpu	cpu for response	cpu for grads.	cpu per grad.
example 1	265.0	178.0	87.0	29.0
example 2	24.0	5.4	18.7	0.9

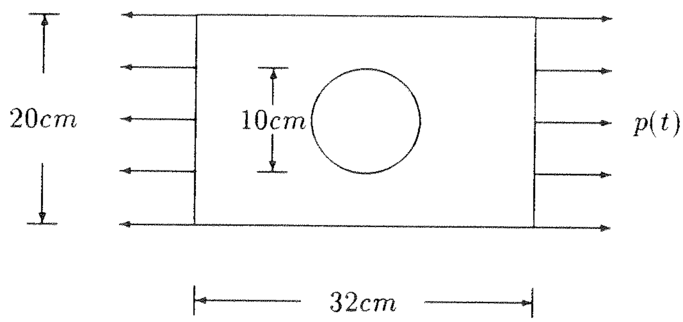

Figure 1: Perforated Strip Under Uniaxial Loading

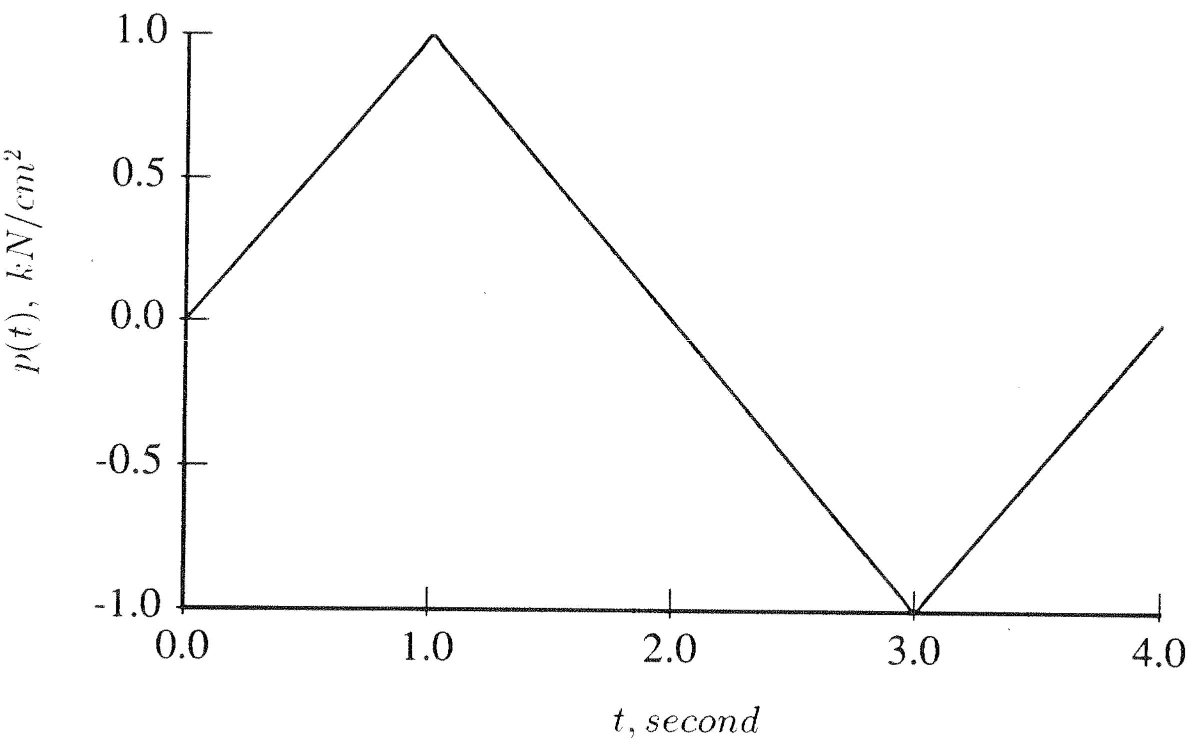

Figure 2: Load $p(t)$ on Perforated Strip

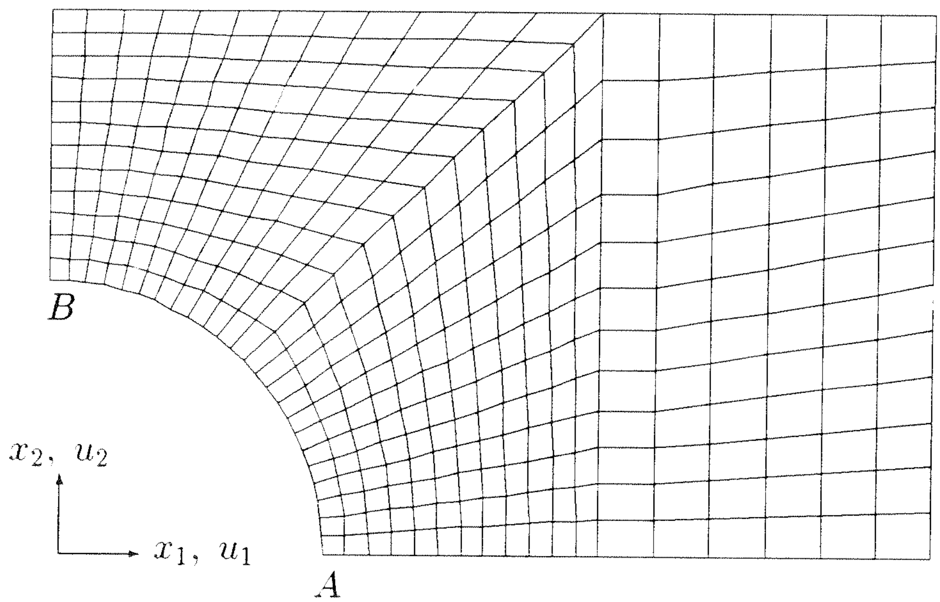

Figure 3: Finite Element Mesh for Perforated Strip

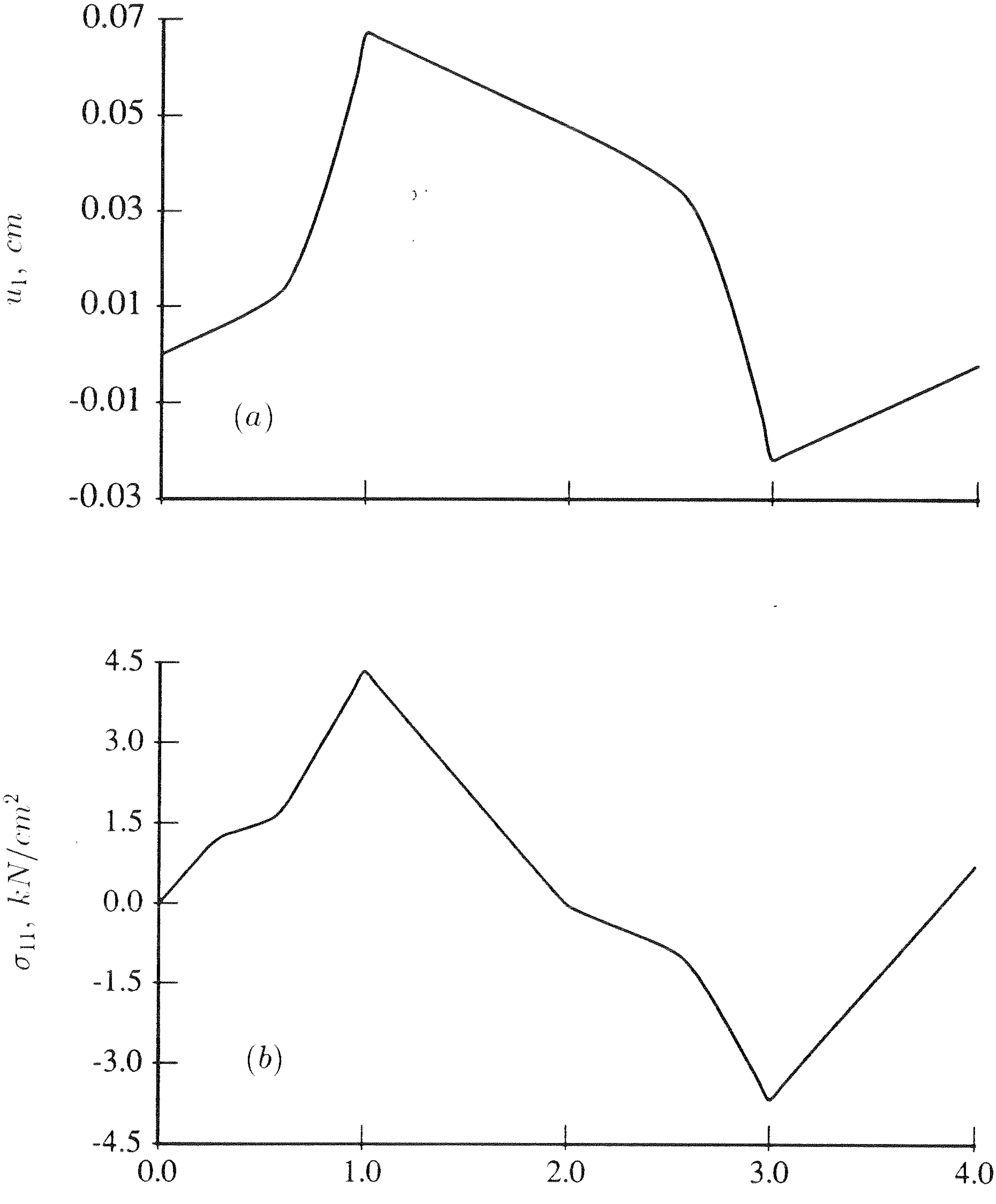

Figure 4: Responses of Perforated Strip: (a) Displacement u_1 at A; (b) Stress σ_{11} at B.

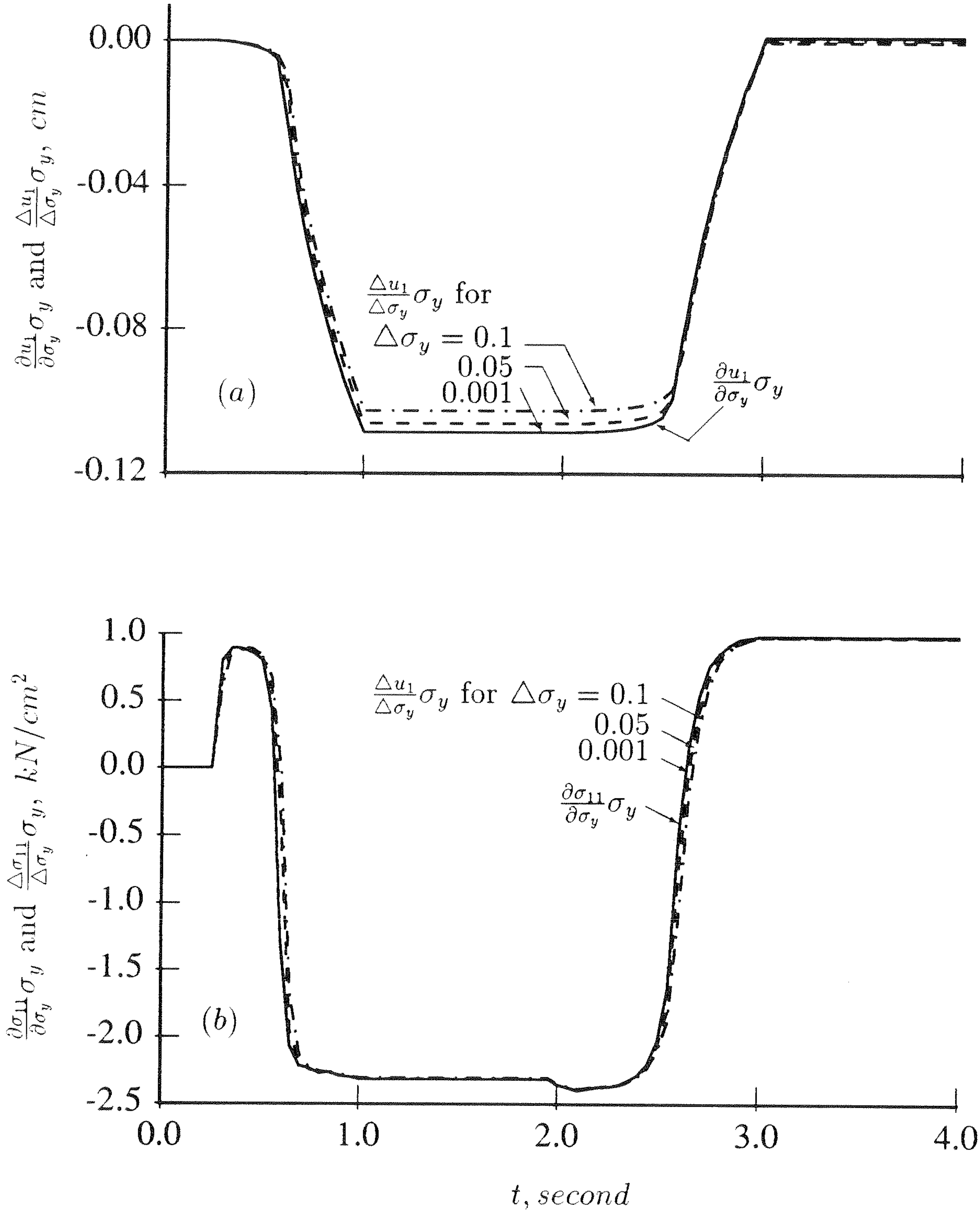

Figure 5: Response Gradients by CDM and by Finite Difference: (a) $\frac{\partial u_1}{\partial \sigma_y}\sigma_y$ and $\frac{\Delta u_1}{\Delta \sigma_y}\sigma_y$ at A; (b) $\frac{\partial \sigma_{11}}{\partial \sigma_y}\sigma_y$ and $\frac{\Delta \sigma_{11}}{\Delta \sigma_y}\sigma_y$ at B.

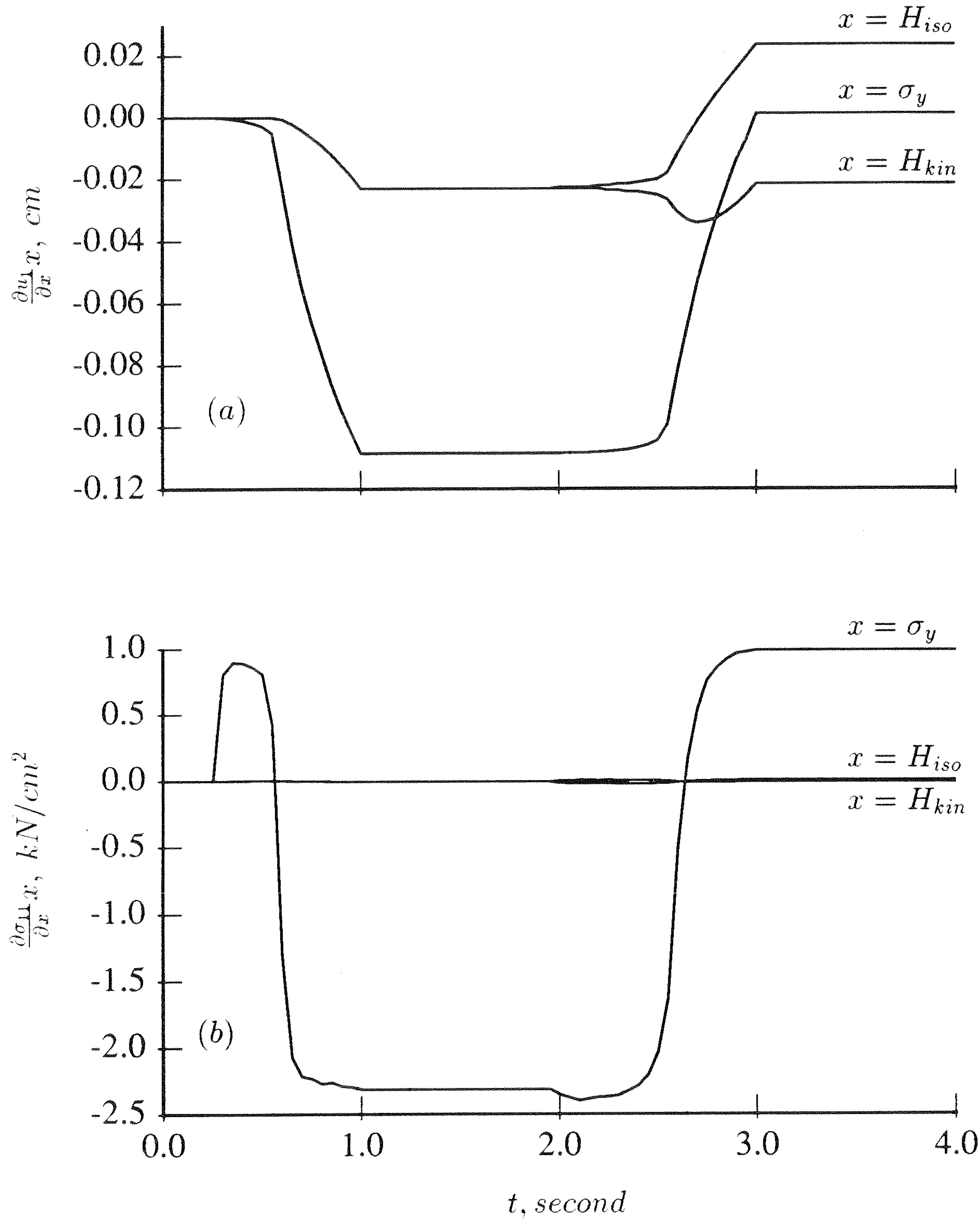

Figure 6: Sensitivities with Respect to σ_y, H_{kin} and H_{iso}: (a) Sensitivities of u_1 at A; (b) Sensitivities σ_{11} at B.

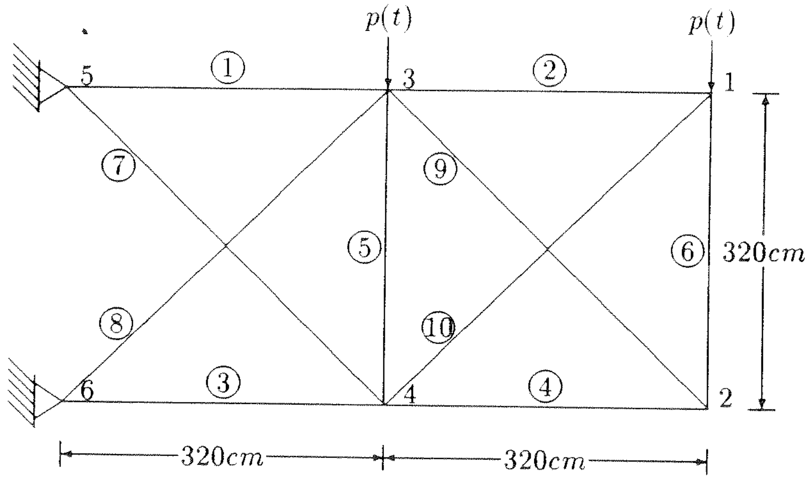

Figure 7: Truss Under Dynamic Loading

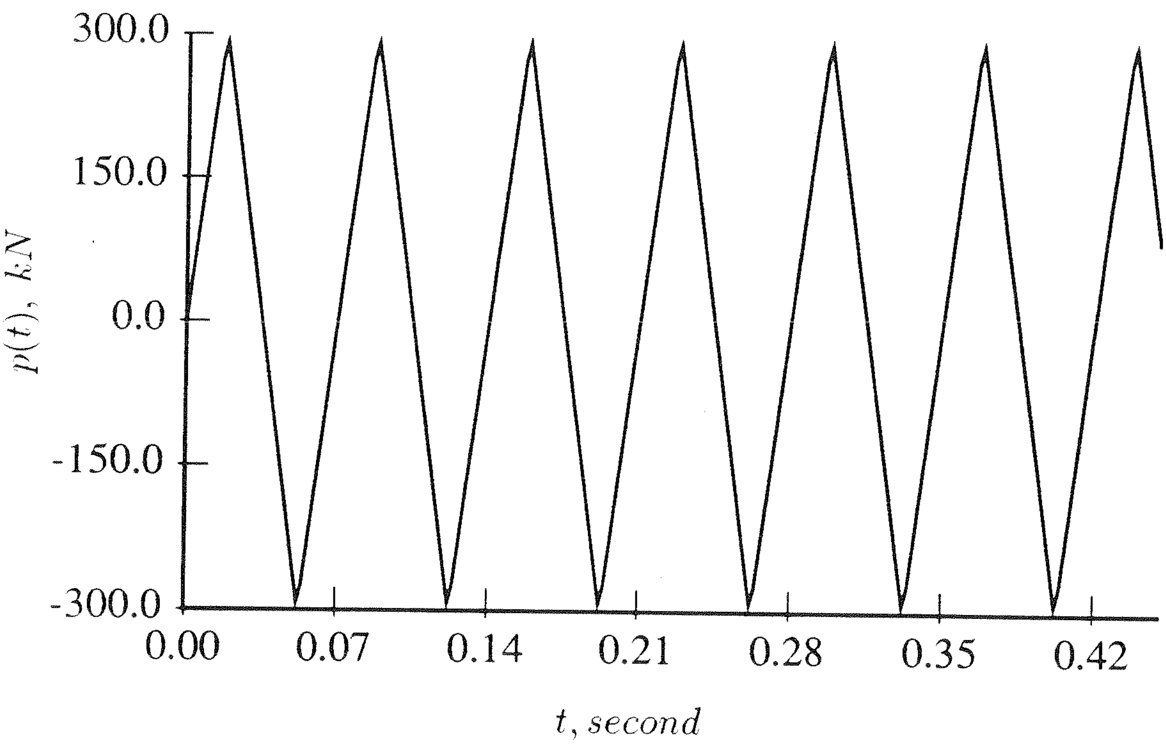

Figure 8: Load $p(t)$ on Truss

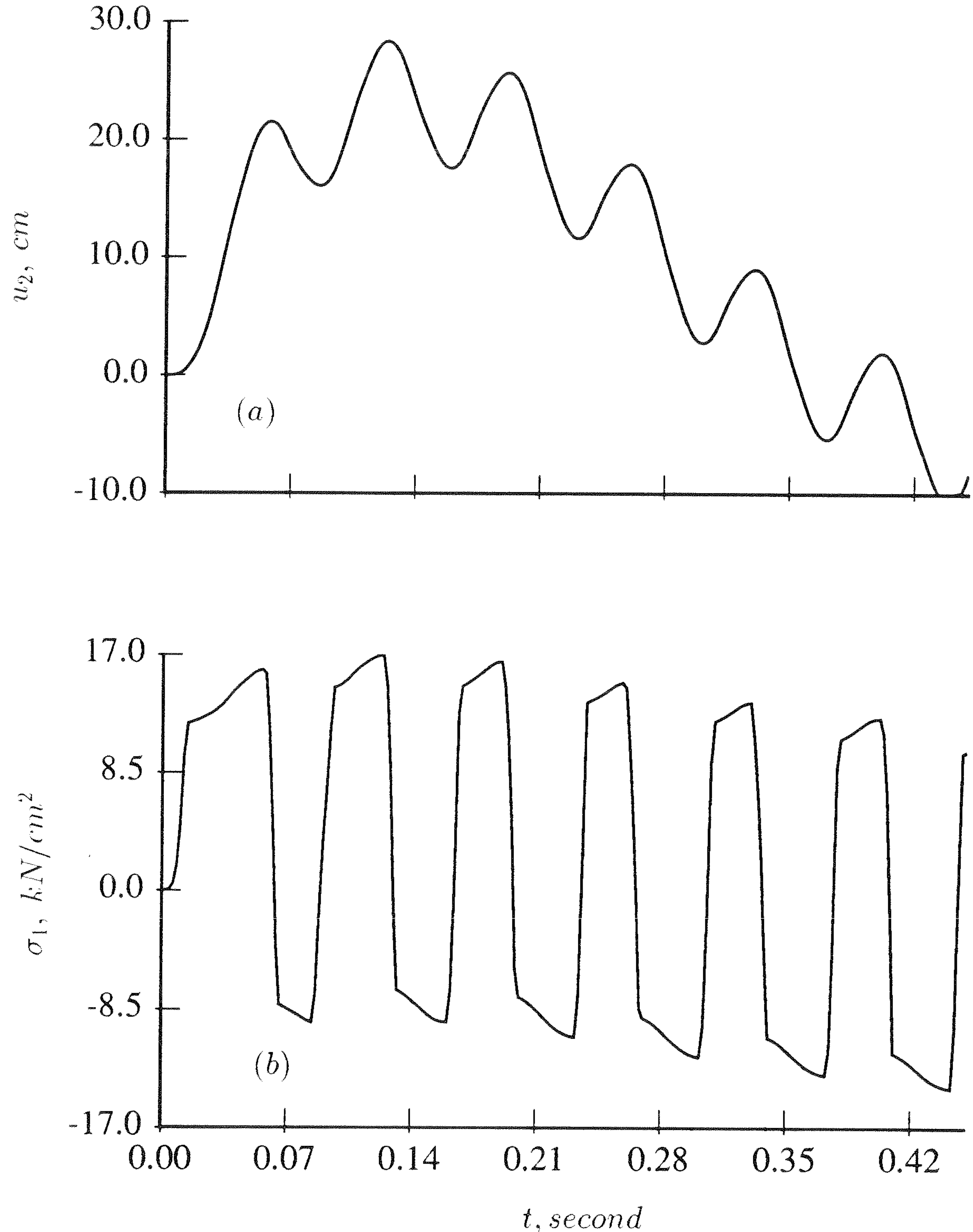

Figure 9: Responses of Truss Structure: (a) Vertical Displacement at Node 2; (b) Stress of Element 1.

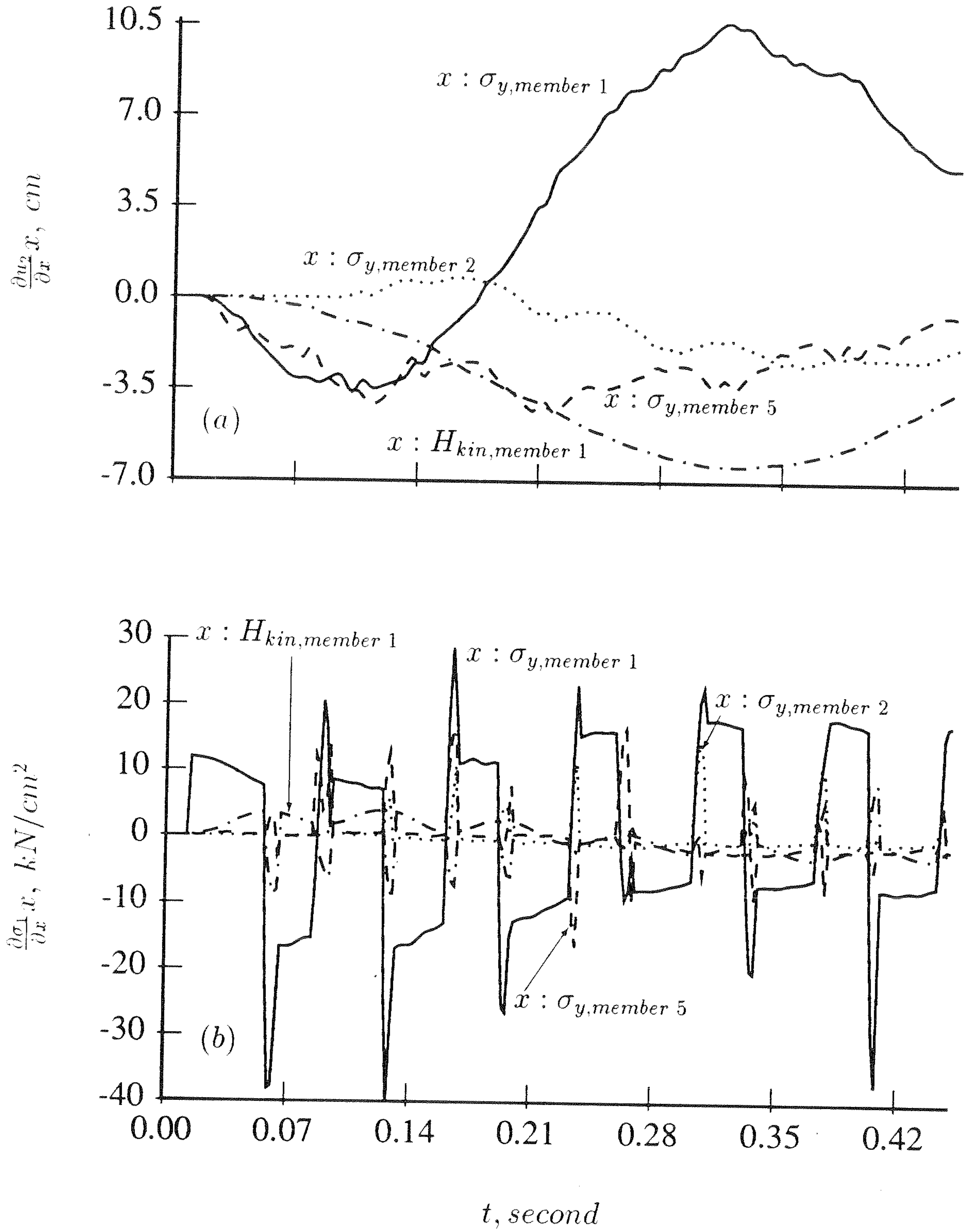

Figure 10: Response Sensitivities of Truss Structure: (a) Sensitivities of Vertical Displacement at Node 2; (b) Sensitivities of Stress of Element 1.